JOC The Journal of Organic Chemistry



Article

# Fluorescence enhancement of aromatic macrocycles by lowering excited singlet state energies

Koki Ikemoto, Toshiki Tokuhira, Akari Uetani, Yu Harabuchi, Sota Sato, Satoshi Maeda, and Hiroyuki Isobe

*J. Org. Chem.*, **Just Accepted Manuscript** • DOI: 10.1021/acs.joc.9b02379 • Publication Date (Web): 06 Nov 2019



is published by the American Chemical Society. 1155 Sixteenth Street N.W., Washington, DC 20036

# Fluorescence enhancement of aromatic macrocycles by lowering excited singlet state energies

Koki Ikemoto,[†,‡] Toshiki Tokuhira,[†] Akari Uetani,[§] Yu Harabuchi,[§,∥,⊥] Sota Sato,[†,‡] Satoshi Maeda,[§,⊥,#] Hiroyuki Isobe[†,‡,*]

[†]Department of Chemistry, The University of Tokyo, Hongo 7-3-1, Bunkyo-ku, Tokyo, 113-0033, Japan

[‡]JST, ERATO Isobe Degenerate π-Integration Project, Hongo 7-3-1, Bunkyo-ku, Tokyo, 113-0033, Japan

[§]Department of Chemistry, Faculty of Science, Hokkaido University, Kita 10, Nishi 8, Kita-ku, Sapporo 060-0810, Japan

[∥]JST, PRESTO, 4-1-8 Honcho, Kawaguchi, Saitama, 332-0012, Japan

[⊥]Institute for Chemical Reaction Design and Discovery (WPI-ICReDD), Hokkaido University, Sapporo 001-0021, Japan

[#]Research and Services Division of Materials Data and Integrated System (MaDIS), National Institute for Materials Science (NIMS), Tsukuba 305-0044, Japan

[*]E-mail: isobe@chem.s.u-tokyo.ac.jp

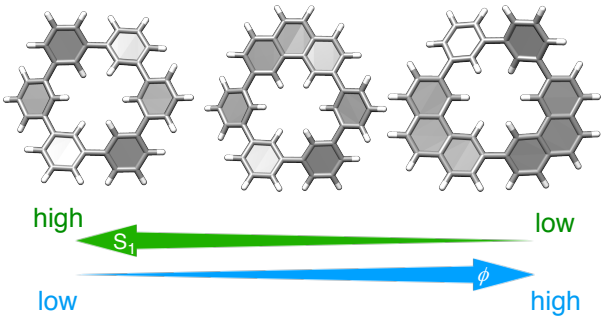


## Abstract

A series of cyclo-*meta*-phenylene congeners with a variation of interphenylene bridges were synthesized by adopting concise synthetic routes to investigate the structure-fluorescence relationships

of macrocycles. With fundamental UV-vis absorption and fluorescence spectra, no unique effect of the macrocyclic structures was noted. However, the fluorescence quantum yields were dramatically affected by the macrocyclic structures and varied at a range of 5–92%. The quantum yields qualitatively depended on the number of the vinylene-bridged phenanthrenylene panels, and the theoretical investigations revealed the energetic and structural effects of the phenanthrenylene panels during nanosecond photodynamic processes. A high energy barrier along the $S_0/S_1$-internal conversion path to reach the minimum energy conical intersection (MECI) was necessary to hamper a non-radiative process, and with the transition state energy level of the excited singlet state being insensitive to macrocyclic structures, a low energy level of excited singlet states ($S_{1MIN}$) was required to facilitate efficient fluorescence.

## Introduction

Manipulating the fluorescence properties of organic molecules holds promise for the development of optical/optoelectronic organic materials. A unique series of organic materials have been designed simply by arraying aromatic panels in macrocyclic structures.[1] For instance, the circularly polarized luminescence of organic molecules was dramatically enhanced by an intense magnetic transient dipole moment induced in belt-persistent macrocycles,[2] and a magnetic-field-induced enhancement of electroluminescence, *i.e.*, a magneto-electroluminescence effect, was observed with [*n*]cyclo-*meta*-phenylene ([*n*]CMP, $n = 6$; Figure 1) embedded in a single-layer organic light-emitting device (OLED).[3,4] Furthermore, a single-layer OLED with a high internal quantum efficiency was fabricated by using solely hydrocarbon macrocycles including [3]cyclo-3,6-phenanthrenylene ([3]CPhen$_{3,6}$) as an efficient emitter.[5,6] However, the structural factors of macrocycles for efficient fluorescence have not been elucidated. Specifically, [6]CMP is a poor emitter with a photoluminescent quantum yield ($\phi$) of 6%, whereas its vinylene-bridged congener, [3]CPhen$_{3,6}$, is an excellent emitter with an efficient yield of $\phi = 75\%$ (Figure 1).[6] However, our understanding of the structure-fluorescence relationships of macrocycles is still immature, and the origins of such

considerable differences in $\phi$ values are unclear. In this study, we designed and synthesized a series of [6]CMP-related macrocycles that differed in the number of phenylene/phenanthrenylene panels having different degrees of π-conjugation and flexibility. The macrocycles also differed in their photoluminescence quantum yields. With the aid of theoretical investigations, the energy levels of excited singlet states were found to be important for facilitating the fluorescence of the macrocycles.

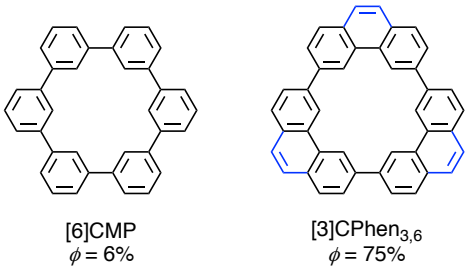


**Figure 1**. Macrocyclic congeners with different bridges. The fluorescence of [6]CMP and its vinylene-bridged congener, [3]CPhen$_{3,6}$, is considerably different.

## Results and discussion

### Synthesis

The structures of the [6]CMP-related macrocycles were diversified by devising a concise, two-step synthetic route. For the two-step synthesis to exploit structural variations between [6]CMP and [3]CPhen$_{3,6}$, three types of coupling components (**1a-1c**) were designed with two phenylene units differing in-between bridges (Scheme 1). Two different coupling components were then assembled into a linear precursor **3** by Suzuki-Miyaura coupling between **1** and **2**,[7] and the macrocyclic structure of a bridged [6]CMP congener **4** was completed by a subsequent Yamamoto-type coupling reaction.[8,9] Six macrocycles with different bridging structures (**4a-4f**) were thus prepared in moderate yields.

**Scheme 1.** Two-step synthesis of [6]CMP-related macrocycles

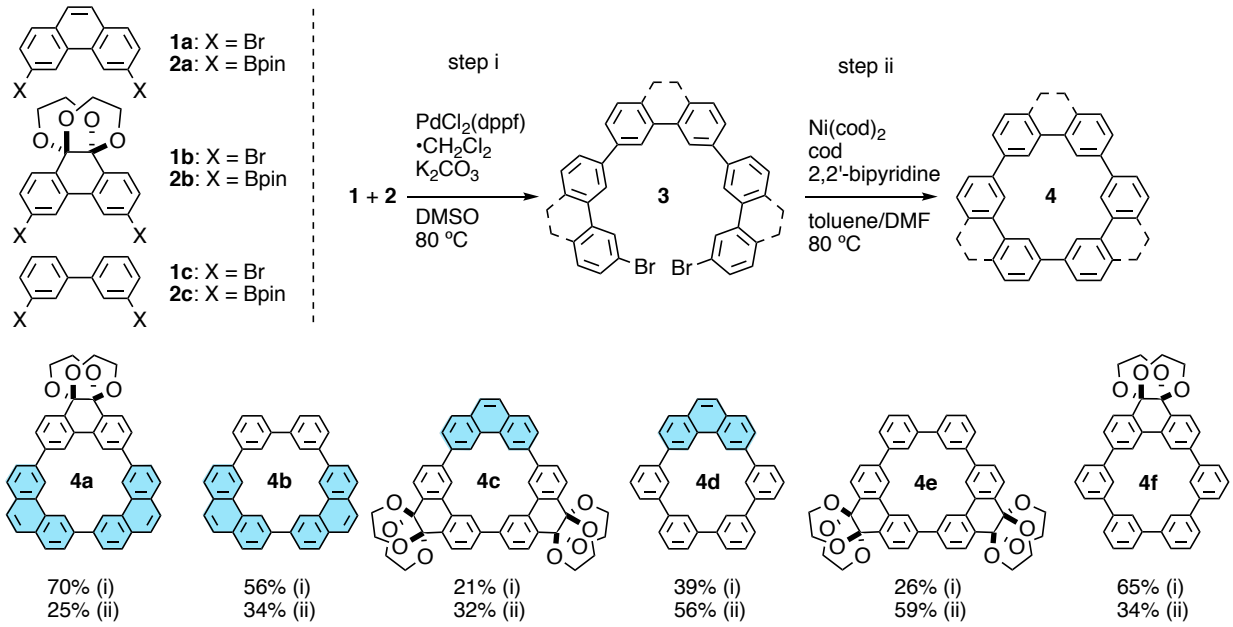


Other relevant compounds were synthesized by adopting different methods. One-pot cyclization of dibromide **1b** with a Yamamoto-type coupling reaction afforded a macrocycle (**4g**) furnished with three methylene/acetal bridges (Scheme 2a).[6, 10] Macrocycle **6** was designed by replacing one two-phenylene unit with one alkane chain. Macrocycle **6** was synthesized from 1,5-hexadiene, which was hydroborylated and coupled with **1a** for the final Ni-mediated cyclization (Scheme 2b).

**Scheme 2.** Synthesis of [6]CMP-related compounds

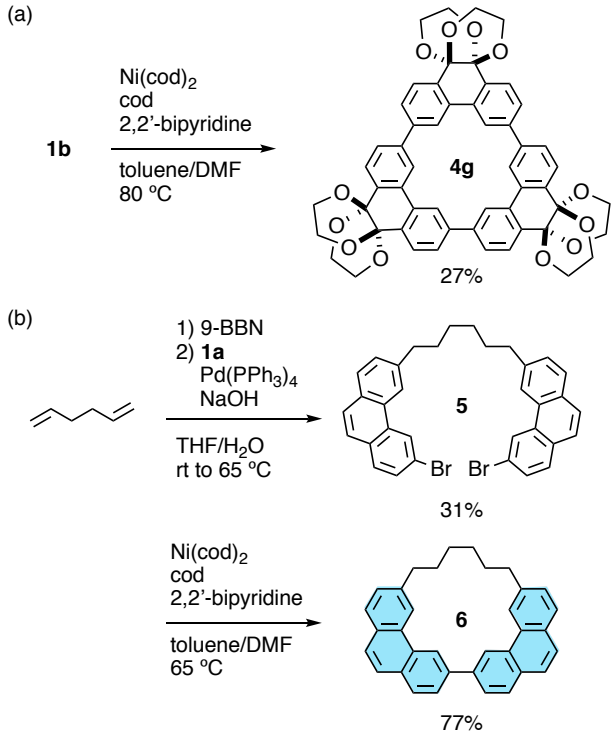


## Photophysical properties

We first measured the UV-vis absorption spectra of the macrocycles and reference compounds. The onset absorption peaks are listed in Table 1 (see also Figure S1 for the spectra).[11] In the presence of phenanthrenylene panels, the absorptions were red-shifted. The observations should be due to the effects of π-extension via vinylene bridges, because the π-extension should narrow the HOMO-LUMO gap and, consequently, lower the excited state energy level (see below). We then measured the fluorescence spectra. As expected, we also observed red-shifted fluorescence peaks with π-extended congeners (Table 1 and Figure S1). However, when we measured the $\phi$ values of the fluorescence, we unexpectedly observed considerable differences among these molecules. Thus, the macrocycles with two or more phenanthrenylene panels exhibited high $\phi$ values above 60% ([3]CPhen$_{3,6}$, **4a**, **4b** and **6**), and the macrocycles without phenanthrenylene panels exhibited low $\phi$ values less than 10% (**4e**, **4f** and **4g**). The highest $\phi$ value was 92% with **4b**, which surpassed the previous value of fluorescent [3]CPhen$_{3,6}$ (75%). A borderline case was the macrocyles with one phenanthrenylene panel:

macrocycle **4d** with one vinylene bridge was a poor emitter with $\phi$ = 27%, and macrocycles **4c** with one vinylene bridge and two methylene/acetal bridges was a good emitter with $\phi$ = 63%.

**Table 1.** Photophysical data. See Figure S1 for the spectra.

| | $\lambda_{abs,onset}$ (nm) | $\lambda_{abs,max}$ (nm), ($\varepsilon$) | $\lambda_{em}$ (nm) | $\phi$ [c] |
|---|---|---|---|---|
| [3]CPhen$_{3,6}$ | 395 [a] | 323 (47,000), 336 (74,000), 375 (14,000) [a] | 396, 419, 445 [a] | 75% [a] |
| **4a** | 402 [a] | 307 (38,000), 321 (51,000), 366 (10,000) [a] | 398, 421, 447 [a] | 78% [a] |
| **4b** | 392 [a] | 315 (41,000), 355 (12,000) [a] | 391, 414, 438 [a] | 92% [a] |
| **4c** | 392 [a] | 339 (22,000), 353 (16,000) [a] | 388 [a] | 63% [a] |
| **4d** | 371 [a] | 333 (17,000), 343 (12,000) [a] | 382, 393 [a] | 27% [a] |
| **4e** | 323 [b] | 260 (14,000) [b] | 347, 355 [b] | 5% [b] |
| **4f** | 319 [b] | 255 (12,000) [b] | 351 [b] | 5% [b] |
| **4g** | 333 [a] | 300 (15,000) [a] | 343, 356 [a] | 8% [a] |
| [6]CMP | 317 [b] | 251 (81,000) [b] | 337, 348 [b] | 6% [b] |
| **6** | 377 [a] | 336 (24,000) [a] | 376 [a] | 60% [a] |
| phenanthrene | 349 [a] | 295 (12,000) [a] | 350, 367, 386 [a] | 15% [a] |

[a] Solvent = toluene. [b] Solvent = $CHCl_3$. [c] Absolute photoluminescence quantum yields were measured on Hamamatsu Photonics C9920-02G.

**Theoretical calculation**

Experimentally, the photoluminescence decay of [3]CPhen$_{3,6}$ was first measured to find a nanosecond-order decay (6.5 nsec) (Figure S2). To gain insights into such nanosecond processes, we then investigated relevant excited-state processes of two representative macrocycles, [6]CMP and [3]CPhen$_{3,6}$, with time-dependent density functional theory (TDDFT). In principle, the excited energy gained at the $S_1$ excited state is consumed *via* two paths leading to the $S_0$ ground state, *i.e.*, a radiative path and a non-radiative path, and the non-radiative path is further categorized into two paths: an $S_0/S_1$-

internal conversion path and singlet-triplet intersystem crossing path. In an internal conversion process, nonadiabatic transitions take place efficiently in conical intersection (CI) regions where two electronic states are energetically degenerate.[12] The lowest energy point within a CI hyperspace, i.e. a minimum energy CI (MECI), is optimized as a representative geometry of a CI region. In a series of investigations, a pivotal role of $S_0/S_1$-internal conversion path has been disclosed for small polyaromatic hydrocarbons (PAHs) by theoretical explorations of the MECIs between the ground and first singlet excited electronic states ($S_0/S_1$-MECIs).[13] However, the applicability of such theoretical models to large molecular materials cannot be taken granted and must be examined at the cost of computational tasks involving many branching paths. In this study, with recent development of automated search protocols adopting the single component-artificial force induced reaction (SC-AFIR) method[14,15] as well as the energy shift (ES)/TDDFT method,[16] we succeeded in locating $S_0/S_1$-MECIs of [6]CMP (60 atoms) and [3]CPhen$_{3,6}$ (66 atoms): there existed 41 $S_0/S_1$-MECIs with [6]CMP and 14 $S_0/S_1$-MECIs with [3]CPhen$_{3,6}$ (Figures S42-S43). Unique structural features of the $S_0/S_1$-MECIs were commonly found with [6]CMP and [3]CPhen$_{3,6}$. Among multiple arylene panels in the macrocycles, only one panel was structurally deformed at the $S_0/S_1$-MECIs, and the deformed structures resembled those of small PAHs with sp$^3$-like deformation localized at one carbon atom (Figure S41).[13]

The $S_0/S_1$-internal conversion path was further clarified by allocating the transition state ($S_{1TS}$) on the $S_1$ surface. The most preferred $S_0/S_1$-paths are shown in Figure 2a and 2b, respectively, for [6]CMP and [3]CPhen$_{3,6}$. The $S_{1TS}$ connecting two minima at the $S_1$ state near the Frank-Condon region ($S_{1MIN}$) and $S_0/S_1$-MECI was located for [6]CMP to reveal an energy barrier of $\Delta E^{\ddagger}$ = 0.42 eV (Figure 2a). The same internal conversion path was also clarified for [3]CPhen$_{3,6}$ to reveal the energy barrier of $\Delta E^{\ddagger}$ = 1.4 eV (Figure 2b). Due to the late transition state for both molecules, the structural deformations at the transition state were similar to those at the $S_0/S_1$-MECI. The deformations at the transition state were therefore localized on a single panel, which resulted in the similar levels of the $S_{1TS}$ energies relative to the $S_{0MIN}$ ground state (5.24 eV for [6]CMP *vs.* 5.00 eV for [3]CPhen$_{3,6}$).[17] Consequently, the energy barrier of the non-radiative $S_0/S_1$-internal conversion is largely determined

by the $S_{1MIN}$ level. The $S_{1MIN}$ energy level of [3]CPhen$_{3,6}$ was 1.22 eV lower than that of [6]CMP, and the lower $S_{1MIN}$ level of [3]CPhen$_{3,6}$ is understood by the stabilization of the π-π* state *via* the delocalization of π and π* orbitals: The delocalization in [3]CPhen$_{3,6}$ is more pronounced by the extended π-conjugation than that in [6]CMP. The observation is consistent with that found in the previous studies.[13,18]

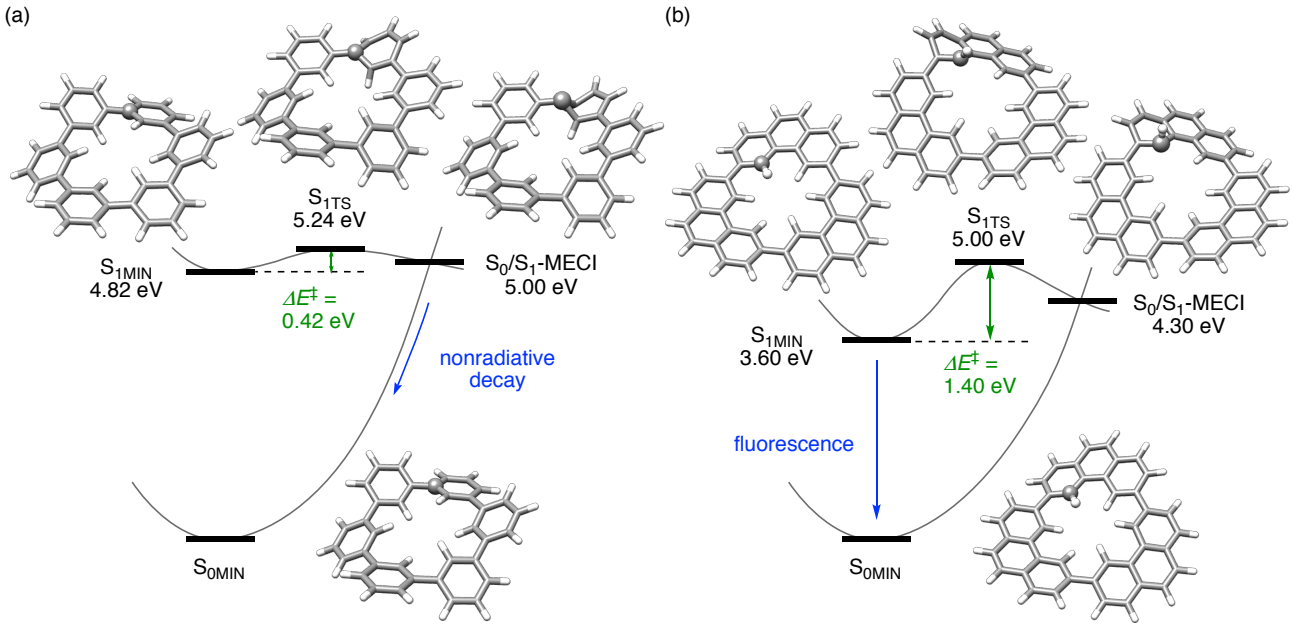


**Figure 2.** Schematic pictures of the energetically most preferred internal conversion path for macrocycles, (a) [6]CMP and (b) [3]CPhen$_{3,6}$. The energy levels of $S_{1MIN}$, $S_{1TS}$ and $S_0/S_1$-MECI at the TDDFT level are shown relative to $S_{0MIN}$ in eV.

Finally, the $S_{1MIN}$ energy levels were theoretically located for all the macrocycles to reveal qualitative correlations with the experimental $\phi$ values. The $S_{1MIN}$ structures for **4a-4g**, **6** and phenanthrene were thus obtained by an identical TDDFT method, and the $S_{1MIN}$ energies relative to the $S_{0MIN}$ energy were plotted against the experimental $\phi$ values (Figure 3). Macrocycles with $S_{1MIN}$ located above 3.6 eV reached $\phi$ values of >70%, and the highest $\phi$ value of 92% was achieved by **4b** with $S_{1MIN}$ = 3.7 eV.[19] The plot qualitatively showed that a higher level of $S_{1MIN}$ above 4 eV resulted

in poor fluorescence, partly because the $S_{1TS}$ levels were not much affected by the molecular structures; the higher the $S_{1MIN}$ is, the lower the potential energy barrier gets along the internal conversion path.[13] As can be found with **4c** and **4d**, the $S_{1MIN}$ at approximately 4 eV should be the borderline, which requires in-depth analysis of $S_{1TS}$ level for speculation about the fluorescence efficiency. In-depth understanding of another important non-radiative path, *i.e.*, intersystem crossing path, should further allow us predict the fluorescence efficiency in a more quantitative manner, which is of current interest for the state-of-the-art theoretical investigations.

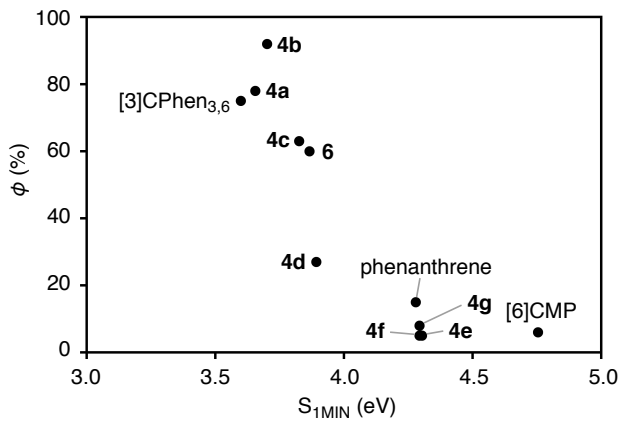


**Figure 3.** Correlations between the $\phi$ values and the $S_{1MIN}$ levels.

## Conclusions

We designed and synthesized a series of macrocycles by assembling phenanthrenylene-related panels, which allowed us to explore the structure-fluorescence relationships of the macrocycles. Among the 10 congeners, one congener with two phenanthrenylene panels and two phenylene panels achieved a remarkable fluorescence quantum yield of 92%. Although we observed the expected red-shifts in UV-vis absorption and fluorescence spectra, the quantum yields of fluorescence unexpectedly varied. With the aid of theoretical studies and the adoption of the state-of-the-art analysis of nanosecond dynamics, we found that the energy barriers for the non-radiative processes determined the quantum yields. With the $S_{1TS}$ levels maintained throughout the macrocyclic congeners, the $S_{1MIN}$ levels decided the energy barrier height along the $S_0/S_1$-internal conversion path. Consequently,

lowering $S_{1MIN}$ level facilitates the efficient fluorescence. We believe that the structure-fluorescence relationships, together with mechanistic insights, can help the future development of fluorescent macrocycles and that optoelectronic macrocyclic materials can be generated to be used in devices.

## Experimental section

**General.** All the reactions were performed under $N_2$ atmosphere. An oil bath was used to elevate the temperature of reactions. Flash silica gel column chromatography was performed on silica gel 60N (spherical and neutral gel, 40–50 μm, Kanto). Gel permeation chromatography (GPC) was performed on a Japan Analytical Industry LC-9104 with JAIGEL 1H-40, 2H-40, and 2.5H-40 polystyrene columns (40 mm i.d. × 600 mm) and chloroform as the eluent. Analytical high pressure liquid chromatography (HPLC) was performed on a JASCO LC-2000 Plus series systems with a COSMOSIL $5C_{18}$-MS-II column (4.6 mm i.d. × 250 mm) and a COSMOSIL π-NAP column (4.6 mm i.d. × 250 mm) with a flow rate of 1.0 mL/min and temperature of 40 °C in a column oven (JASCO CO-2060PLUS) while under observation with a UV-vis detector (JASCO MD2018PLUS). Proton ($^1$H) and carbon ($^{13}$C) NMR spectra were recorded at 298 K on a JEOL RESONANCE JNM-ECA II 600 equipped with the UltraCOOL probe. Chemical shift values are given in ppm with relative to residual solvent signals of chloroform ($^1$H NMR: $\delta$ 7.26; $^{13}$C NMR: $\delta$ 77.2). Data are reported as follows: chemical shift, multiplicity (s = singlet, brs = broad singlet, d = doublet, t = triplet, m = multiplet), coupling constant in hertz (Hz) and a relative integration value. High-resolution mass spectrometry was performed on a Bruker micrOTOF II spectrometer equipped with an APCI probe. Elemental analyses were performed on an ELEMENTAR Vario MICRO cube (Elemental Analysis Center, School of Science, The University of Tokyo). As was the case with large macrocycles,[4,10] removal of solvent was not feasible with the present macrocycles. Ultraviolet-visible (UV) spectra were recorded on a JASCO V-670 spectrometer. Fluorescence spectra were recorded on a JASCO FP-8500 spectrophotometer. Absolute fluorescence quantum yields were determined on a Hamamatsu Quantaurus-QY C11347.

Anhydrous THF, DMF and toluene were purified by a solvent purification system (GlassContour) equipped with columns of activated alumina and supported copper catalyst (Q-5). The 3,6-dibromophenanthrene (**1a**)[20] and compound **1b**[21] were synthesized according to literature procedures.

**Synthesis.**

*3,6-Diborylphenanthrene **2a***: A mixture of 3,6-dibromophenanthrene (**1a**) (1.00 g, 2.98 mmol), $PdCl_2(dppf)\bullet CH_2Cl_2$ (286 mg, 0.595 mmol), bis(pinacolato)diboron (2.27 g, 8.93 mmol) and potassium acetate (1.46 g, 14.9 mmol) in 1,4-dioxane (30 mL) was stirred at 80 ºC for 15 h. After addition of water (30 mL), the aqueous layer was extracted with $CHCl_3$ (30 mL × 3), and the combined organic layer was washed with brine (120 mL), dried over $Na_2SO_4$, and concentrated in vacuo. The crude mixture was washed with MeOH (30 mL) to afford the title compound as an off-white powder in 89% yield (1.14 g, 2.64 mmol). The spectra of **2a** were identical to data found in the literature.[22]

*Diboryl acetal **2b***: A mixture of compound **1b** (2.13 g, 4.70 mmol), $PdCl_2(dppf)\bullet CH_2Cl_2$ (192 mg, 0.235 mmol), bis(pinacolato)diboron (2.63 g, 10.4 mmol) and potassium acetate (2.77 g, 28.2 mmol) in 1,4-dioxane (47 mL) was stirred at 80 ºC for 20 h. After addition of water (50 mL), the aqueous layer was extracted with $CHCl_3$ (50 mL × 3), and the combined organic layer was washed with brine (180 mL), dried over $Na_2SO_4$, and concentrated in vacuo. The crude mixture was washed with MeOH (100 mL) to afford the title compound as an off-white powder in 94% yield (2.43 g, 4.42 mmol). $^1$H NMR (600 MHz, $CDCl_3$) $\delta$ 8.41 (s, 2H), 7.87 (d, $J$ = 7.5, 0.9 Hz, 2H), 7.74 (d, $J$ = 7.5 Hz, 2H), 4.20 (brs, 4H), 3.65 (brs, 4H), 1.39 (s, 24H); $^{13}$C{$^1$H} NMR (150 MHz, $CDCl_3$) $\delta$ 135.6, 135.3, 132.7, 130.6, 125.4, 92.8, 84.2, 61.6, 25.0 (A signal for the carbon nuclei bonded to the boron nuclei was not observed due to the quadrupolar relaxation induced by the boron nuclei.); HRMS (APCI/TOF) $m/z$ $[M + H]^+$ calcd for $C_{30}H_{39}B_2O_8$ 549.2826, found 549.2831.

*3,3'-Diboryl-1,1'-biphenyl (**2c**)*: A mixture of 3,3'-dibromo-1,1'-biphenyl (**1c**) (3.12 g, 10.0 mmol), $PdCl_2(PPh_3)_2$ (351 mg, 0.500 mmol), bis(pinacolato)diboron (5.59 g, 22.0 mmol) and potassium acetate (4.91 g, 50.0 mmol) in DMSO (50 mL) was stirred at 80 ºC for 18 h. After addition

of water (80 mL), the precipitate was collected by filtration and washed with water (20 mL). The solid was dissolved in AcOEt (80 mL), and the organic layer was washed with brine (100 mL), dried over $Na_2SO_4$, and concentrated in vacuo. The crude mixture was purified by silica gel column chromatography (eluent: AcOEt:hexane = 1:10) to afford the title compound as an off-white powder in 97% yield (3.96 g, 9.74 mmol). Spectra of **2c** were identical to data found in the literature.[23]

**Two-step Syntheses of [6]CMP-related Macrocycles.**

*5,10 - bis(6 - bromophenanthren - 3 - yl) - 15,18,19,22 - tetraoxapentacyclo[12.4.4.0$^{1,14}$.0$^{2,7}$.0$^{8,13}$]docosa - 2(7),3,5,8(13),9,11 - hexaene (Precursor **3a**)*: A mixture of diboryl acetal **2b** (206 mg, 0.376 mmol), 3,6-dibromophenanthrene (**1a**) (631 mg, 1.88 mmol), $PdCl_2$(dppf)•$CH_2Cl_2$ (30.7 mg, 0.0376 mmol) and potassium carbonate (260 mg, 1.88 mmol) in DMSO (7.5 mL) was stirred at 80 ºC for 24 h. After addition of water (15 mL), the resulting precipitate was collected by filtration and washed with water (10 mL) and MeOH (10 mL). The crude material was purified by silica gel column chromatography (eluent: chloroform) and gel permeation chromatography to afford the title compound in 70% yield (211 mg, 0.262 mmol) as a white solid. $R_f$ = 0.59 (chloroform); $^1$H NMR (600 MHz, $CDCl_3$) $\delta$ 8.88 (d, $J$ = 1.8 Hz, 2H), 8.82 (d, $J$ = 1.2 Hz, 2H), 8.37 (d, $J$ = 1.5 Hz, 2H), 8.00 (d, $J$ = 8.1 Hz, 2H), 7.98 (d, $J$ = 8.1 Hz, 2H), 7.94 (dd, $J$ = 8.1, 1.2 Hz, 2H), 7.87 (dd, $J$ = 8.1, 1.5 Hz, 2H), 7.79 (d, $J$ = 8.7 Hz, 2H), 7.77 (d, $J$ = 8.4 Hz, 2H), 7.71 (d, $J$ = 8.7 Hz, 2H), 7.69 (dd, $J$ = 8.4, 1.8 Hz, 2H), 4.33 (brs, 4H), 3.81 (brs, 4H); $^{13}$C NMR (150 MHz, $CDCl_3$, 298 K) $\delta$ 143.4, 139.7, 133.7, 132.5, 131.9, 131.8, 131.0, 130.3, 130.1, 129.6, 129.4, 128.6, 127.2, 127.2, 126.9, 126.8, 125.8, 123.7, 121.6, 121.2, 92.9, 61.7. HRMS (APCI/TOF) $m/z$ $[M + H]^+$ calcd for $C_{46}H_{31}Br_2O_4$ 805.0584, found 805.0560.

*27,30,39,42 - Tetraoxadodecacyclo[20.12.4.4$^{26,31}$.2$^{2,5}$.2$^{8,11}$.2$^{12,15}$.2$^{18,21}$.0$^{4,9}$.0$^{14,19}$.0$^{25,37}$.0$^{26,31}$.0$^{32,36}$]pentaconta - 1(35),2,4,6,8,10,12,14,16,18,20,22(38),23,25(37),32(36),33,43,45,47,49 - icosaene (Macrocycle **4a**)*: After stirring mixture of 2,2'-bipyridine (168 mg, 1.08 mmol), 1,5-cyclooctadiene (132 µL, 10.8 mmol) and bis(1,5-cyclooctadiene)nickel(0) (296 mg, 1.08 mmol) in a mixture of toluene (2.3 mL)

and DMF (2.3 mL) at 80 ºC for 30 min, a solution of precursor **3a** (109 mg, 0.135 mmol) in toluene (9 mL) was added dropwise over 1 h. The mixture was stirred at 80 °C for an additional 1 h. After the reaction mixture was cooled down to ambient temperature, water (13 mL) was added, and the mixture was stirred vigorously overnight. The precipitate was collected by filtration and washed with water (10 mL) and MeOH (10 mL). Recrystallization from *o*-dichlorobenzene gave the title compound in 25% yield (23 mg, 0.034 mmol) as a white solid. $^1$H NMR (600 MHz, $CDCl_3$) $\delta$ 9.93 (s, 2H), 9.80 (s, 2H), 9.12 (s, 2H), 8.24 (dd, $J$ = 7.8, 1.8 Hz, 2H), 8.14 (dd, $J$ = 8.4, 1.8 Hz, 2H), 8.10 (dd, $J$ = 8.1, 1.8 Hz, 2H), 8.01 (d, $J$ = 7.8 Hz, 2H), 8.00 (d, $J$ = 8.4 Hz, 2H), 7.91 (d, $J$ = 8.1 Hz, 2H), 7.78 (d, $J$ = 8.7 Hz, 2H), 7.77 (d, $J$ = 8.7 Hz, 2H), 4.32 (brs, 4H), 3.78 (brs, 4H); The $^{13}$C NMR spectrum was not obtained owing to low solubility of the title compound; HRMS (APCI/TOF) $m/z$ $[M + H]^+$ calcd. for $C_{46}H_{31}O_4$ 647.2217, found 647.2198. Anal. Calcd for $(C_{46}H_{30}O_4)_1(C_6H_4Cl_2)_{0.1}$: C 84.62, H 4.63, Cl 1.07. Found, C 84.45, H 4.70, Cl 1.26. The assignment is supported by an X-ray crystallographic structure determination.

*3 - Bromo - 6 - [3′ - (6 - bromophenanthren - 3 - yl) - [1,1′ - biphenyl] - 3 - yl]phenanthrene (Precursor **3b**)*: Following the procedure to prepare **3a**, a reaction mixture of **2c** (406 mg, 1.00 mmol) and **1a** (1.68 g, 5.00 mmol) afforded the title compound in 56% yield (370 mg, 0.556 mmol) as a white solid. $R_f$ = 0.31 (chloroform/hexane = 1:4); $^1$H NMR (600 MHz, $CDCl_3$) $\delta$ 8.90 (d, $J$ = 1.8 Hz, 2H), 8.84 (d, $J$ = 1.2 Hz, 2H), 8.08 (dd, $J$ = 1.5, 1.5 Hz, 2H), 8.00 (d, $J$ = 8.4 Hz, 2H), 7.97 (dd, $J$ = 8.4, 1.2 Hz, 2H), 7.82 (ddd, $J$ = 8.4, 1.5, 1.5 Hz, 2H), 7.80 (d, $J$ = 9.0 Hz, 2H), 7.79-7.77 (m, 4H), 7.72-7.67 (m, 6H); $^{13}$C{$^1$H} NMR (150 MHz, $CDCl_3$) $\delta$ 142.2, 142.2, 140.0, 132.0, 131.6, 131.0, 130.4, 130.1, 129.7, 129.7, 129.4, 127.2, 127.0, 127.0, 126.9, 126.8, 126.6, 125.7, 121.5, 121.1; HRMS (APCI/TOF) $m/z$ $[M + H]^+$ calcd for $C_{40}H_{25}Br_2$ 663.0318, found 663.0308.

*Nonacyclo[20.8.4.2$^{2,5}$.2$^{8,11}$.1$^{12,16}$.1$^{17,21}$.0$^{4,9}$.0$^{25,33}$.0$^{28,32}$]tetraconta - 1(31),2,4,6,8,10,12(36),13,15,17,19,21(35),22(34),23,25(33),26,28(32),29,37,39 - icosaene (Macrocycle **4b**)*: Following the reaction procedure to prepare **4a**, the macrocyclization of **3b** (263 mg, 0.396 mmol) afforded the title compound in 34% yield (69.7 mg, 0.135 mmol) as a white

solid after the purification by recrystallization from *o*-dichlorobenzene. $^1$H NMR (600 MHz, $CDCl_3$) $\delta$ 9.87 (s, 2H), 9.64 (s, 2H), 8.65 (s, 2H), 8.25 (dd, $J$ = 8.3, 1.5 Hz, 2H), 8.08 (dd, $J$ = 8.1, 1.8 Hz, 2H), 8.06 (d, $J$ = 8.3 Hz, 2H), 8.03 (d, $J$ = 8.1 Hz, 2H), 7.95 (d, $J$ = 7.8 Hz, 2H), 7.82 (s, 4H), 7.73 (d, $J$ = 7.8 Hz, 2H), 7.65 (dd, $J$ = 7.8, 7.8 Hz, 2H); The $^{13}$C NMR spectrum was not obtained owing to low solubility of the title compound; HRMS (APCI/TOF) $m/z$ $[M + H]^+$ calcd for $C_{40}H_{25}$ 505.1951, found 505.1939. Anal. Calcd for $(C_{40}H_{24})_1(C_6H_4Cl_2)_{0.07}$: C 94.29, H 4.75, Cl 0.96. Found, C 94.26, H 4.70, Cl 0.97.

*5 - Bromo - 10 - (6 - {10 - bromo - 15,18,19,22 - tetraoxapentacyclo[12.4.4.0$^{1,14}$.0$^{2,7}$.0$^{8,13}$]docosa - 2(7),3,5,8(13),9,11 - hexaen - 5 - yl}phenanthren - 3 - yl) - 15,18,19,22 - tetraoxapentacyclo[12.4.4.0$^{1,14}$.0$^{2,7}$.0$^{8,13}$]docosa - 2(7),3,5,8(13),9,11 - hexaene (Precursor **3c**)*: Following the procedure to prepare **3a**, a reaction mixture of **2a** (100 mg, 0.233 mmol) and **1b** (528 mg, 1.16 mmol) afforded the title compound in 21% yield (44 mg, 0.048 mmol) as a white solid. $R_f$ = 0.20 (chloroform); $^1$H NMR (600 MHz, $CDCl_3$) $\delta$ 8.98 (s, 2H), 8.19 (d, $J$ = 1.4 Hz, 2H), 8.15 (d, $J$ = 1.6 Hz, 2H), 8.05 (d, $J$ = 8.4 Hz, 2H), 7.92 (dd, $J$ = 8.4, 1.2 Hz, 2H), 7.91 (d, $J$ = 7.8 Hz, 2H), 7.87 (dd, $J$ = 7.8, 1.4 Hz, 2H), 7.85 (s, 2H), 7.66 (d, $J$ = 8.4 Hz, 2H), 7.56 (dd, $J$ = 8.4, 1.6 Hz, 2H), 4.24 (brs, 8H), 3.69 (brs, 8H); $^{13}$C{$^1$H} NMR (150 MHz, $CDCl_3$) $\delta$ 143.7, 139.2, 135.2, 132.5, 132.4, 132.3, 132.0, 131.9, 130.7, 129.5, 129.0, 128.4, 127.3, 127.2, 127.1, 126.5, 124.6, 123.6, 121.7, 92.6 (2C), 61.6 (2C); HRMS (APCI/TOF) $m/z$ $[M + H]^+$ calcd for $C_{50}H_{37}Br_2O_8$ 923.0850, found 923.0854.

*7,10,31,34,43,46,53,56 - Octaoxatetradecacyclo[24.12.4.4$^{6,11}$.4$^{30,35}$.2$^{2,5}$.2$^{12,15}$.2$^{16,19}$.2$^{22,25}$.0$^{4,13}$.0$^{6,11}$.0$^{18,23}$.0$^{29,41}$.0$^{30,35}$.0$^{36,40}$]octapentaconta - 1(39),2,4,12,14,16,18,20,22,24,26(42),27,29(41),36(40),37,47,49,51,57 - nonadecaene (Macrocycle **4c**)*: Following the reaction procedure to prepare **4a**, the macrocyclization was performed using **3c** (191 mg, 0.207 mmol). The crude mixture was washed with boiling *o*-dichlorobenzene (50 mL), and the residue was then extracted with boiling nitrobenzene (100 mL). After evaporation of nitrobenzene, the material was washed with $CHCl_3$ (10 mL) to afford the title compound in 32% yield

(55 mg, 0.067 mmol) as a white solid. $^1$H NMR (600 MHz, $CDCl_3$) $\delta$ 9.65 (s, 2H), 9.03 (s, 2H), 8.91 (s, 2H), 8.17 (d, $J$ = 8.4, 1.8 Hz, 2H), 8.11 (d, $J$ = 8.1, 1.5 Hz, 2H), 8.03 (d, $J$ = 7.8 Hz, 2H), 8.01 (d, $J$ = 8.1, 1.5 Hz, 2H), 7.93 (d, $J$ = 7.8 Hz, 2H), 7.91 (d, $J$ = 8.4 Hz, 2H), 7.82 (s, 2H), 4.30 (brs, 8H), 3.78 (brs, 8H); The $^{13}$C NMR spectrum was not obtained owing to low solubility of the title compound; HRMS (APCI/TOF) $m/z$ $[M + H]^+$ calcd for $C_{50}H_{37}O_8$ 765.2483, found 765.2504; Anal. Calcd for $(C_{50}H_{36}O_8)_1(C_6H_5NO_2)_{0.4}$: C 77.31, H 4.71, N 0.69. Found, C 77.01, H 4.62, N 0.68.

*3,6‐Bis({3′‐bromo‐[1,1′‐biphenyl]‐3‐yl})phenanthrene (Precursor **3d**)*: Following the procedure to prepare **3a**, a reaction mixture of **2a** (186 mg, 0.432 mmol) and **1c** (673 mg, 2.16 mmol) afforded the title compound in 39% yield (107 mg, 0.167 mmol) as a white solid. $R_f$ = 0.41 (chloroform/hexane = 1:4); $^1$H NMR (600 MHz, $CDCl_3$) $\delta$ 8.96 (d, $J$ = 1.4 Hz, 2H), 8.02 (d, $J$ = 7.7 Hz, 2H), 7.93 (d, $J$ = 1.2 Hz, 2H), 7.90 (dd, $J$ = 7.7, 1.4 Hz, 2H), 7.83 (dd, $J$ = 2.4, 1.9 Hz, 2H), 7.82 (s, 2H), 7.81-7.78 (m, 2H), 7.66-7.60 (m, 6H), 7.51 (ddd, $J$ = 8.1, 1.9, 1.1 Hz, 2H), 7.34 (dd, $J$ = 8.1, 8.1 Hz, 2H); $^{13}$C{$^1$H} NMR (150 MHz, $CDCl_3$) $\delta$ 143.4, 142.5, 140.6, 139.5, 131.8, 130.8, 130.6, 130.5 (2C), 129.7, 129.4, 127.5, 127.0, 126.7, 126.5, 126.4, 126.1, 123.1, 121.4; HRMS (APCI/TOF) $m/z$ $[M + H]^+$ calcd for $C_{38}H_{25}Br_2$ 639.0318, found 639.0304.

*Octacyclo[20.8.4.1$^{2,6}$.1$^{7,11}$.1$^{12,16}$.1$^{17,21}$.0$^{25,33}$.0$^{28,32}$]octatriaconta‐1(31),2(38),3,5,7,9,11(37),12(36),13,15,17,19,21(35),22(34),23,25(33),26,28(32),29‐nonadecaene (Macrocycle **4d**)*: Following the reaction procedure to prepare **4a**, the macrocyclization of **3d** (102 mg, 0.159 mmol) afforded the title compound in 56% yield (43.0 mg, 0.0892 mmol) as a white solid after the purification by recrystallization from *o*-dichlorobenzene. $^1$H NMR (600 MHz, $CDCl_3$) $\delta$ 9.54 (s, 2H), 8.71 (s, 2H), 8.57 (s, 2H), 8.10 (dd, $J$ = 8.3, 1.5 Hz, 2H), 8.02 (d, $J$ = 8.3 Hz, 2H), 7.92 (d, $J$ = 7.8 Hz, 2H), 7.84 (d, $J$ = 7.2 Hz, 2H), 7.81 (s, 2H), 7.80 (d, $J$ =7.8 Hz, 2H), 7.77 (d, $J$ =7.8 Hz, 2H), 7.62 (dd, $J$ = 7.8, 7.2 Hz, 2H), 7.61 (dd, $J$ = 7.8, 7.2 Hz, 2H); The $^{13}$C NMR spectrum was not obtained owing to low solubility; HRMS (APCI/TOF) $m/z$ $[M + H]^+$ calcd for $C_{38}H_{25}$ 481.1951, found 481.1975; Anal. Calcd for $(C_{38}H_{24})_1(C_6H_4Cl_2)_{0.01}$: C 94.83, H 5.03, Cl 0.15. Found, C 94.83, H 4.95, Cl 0.23.

*5‐Bromo‐10‐(3′‐{10‐bromo‐15,18,19,22‐*

*tetraoxapentacyclo[12.4.4.0$^{1,14}$.0$^{2,7}$.0$^{8,13}$]docosa - 2(7),3,5,8(13),9,11 - hexaen - 5 - yl} - [1,1' - biphenyl] - 3 - yl) - 15,18,19,22 - tetraoxapentacyclo[12.4.4.0$^{1,14}$.0$^{2,7}$.0$^{8,13}$]docosa - 2(7),3,5,8(13),9,11 - hexaene (Precursor **3e**)*: Following the procedure to prepare **3a**, a reaction mixture of **2c** (203 mg, 0.500 mmol) and **1b** (1.14 g, 2.50 mmol) afforded the title compound in 26% yield (117 mg, 0.130 mmol) as a white solid. $R_f$ = 0.25 (chloroform); $^1$H NMR (600 MHz, $CDCl_3$) $\delta$ 8.11 (d, $J$ = 1.6 Hz, 2H), 8.07 (d, $J$ = 1.8 Hz, 2H), 7.90 (dd, $J$ = 1.5, 1.5 Hz, 2H), 7.85 (d, $J$ = 8.1 Hz, 2H), 7.74 (dd, $J$ = 8.1, 1.8 Hz, 2H), 7.71 (ddd, $J$ = 7.2, 1.5, 1.5 Hz, 2H), 7.67 (ddd, $J$ = 7.8, 1.5, 1.5 Hz, 2H), 7.65 (d, $J$ = 8.3 Hz, 2H), 7.62 (dd, $J$ = 7.8, 7.2 Hz, 2H), 7.56 (dd, $J$ = 8.3, 1.6 Hz, 2H), 4.23 (brs, 8H), 3.69 (brs, 8H); $^{13}$C{$^1$H} NMR (150 MHz, $CDCl_3$) $\delta$ 143.3, 142.0, 141.5, 135.2, 132.4, 132.4, 132.2, 131.9, 129.6, 128.6, 128.3, 127.2, 127.1, 127.0, 126.7, 126.6, 124.5, 123.3, 92.6 (2C), 61.6 (2C); HRMS (APCI/TOF) $m/z$ [M + H]$^+$ calcd for $C_{48}H_{37}Br_2O_8$ 899.0850, found 899.0872.

*7,10,31,34,43,46,51,54 - Octaoxatridecacyclo[24.12.4.4$^{6,11}$.4$^{30,35}$.2$^{2,5}$.2$^{12,15}$.1$^{16,20}$.1$^{21,25}$.0$^{4,13}$.0$^{6,11}$.0$^{29,41}$.0$^{30,35}$.0$^{36,40}$]hexapentaconta - 1(39),2,4,12,14,16(48),17,19,21,23,25(47),26(42),27,29(41),36(40),37,49,55 - octadecaene (Macrocycle **4e**)*: Following the reaction procedure to prepare **4a**, the macrocyclization of **3e** (90 mg, 0.10 mmol) afforded the title compound in 59% yield (45 mg, 0.059 mmol) as a white solid after the purification by silica gel column chromatography (eluent: chloroform) and gel permeation chromatography. $^1$H NMR (600 MHz, $CDCl_3$) $\delta$ 8.78 (s, 2H), 8.73 (s, 2H), 8.34 (s, 2H), 7.93 (dd, $J$ = 8.1, 1.5 Hz, 2H), 7.89-7.88 (m, 6H), 7.83 (d, $J$ = 7.2 Hz, 2H), 7.71 (d, $J$ = 7.2 Hz, 2H), 7.60 (dd, $J$ = 7.2, 7.2 Hz, 2H), 4.29 (brs, 8H), 3.77 (brs, 8H); $^{13}$C{$^1$H} NMR (150 MHz, $CDCl_3$) $\delta$ 142.2, 141.3, 140.3, 140.0, 133.6, 133.4, 133.1, 132.7, 129.7, 127.3, 127.2, 126.9, 126.6, 126.5, 126.3, 125.2, 122.7, 121.9, 93.0, 93.0, 61.7 (2C); HRMS (APCI/TOF) $m/z$ [M + H]$^+$ calcd for $C_{48}H_{37}O_8$ 741.2483, found 741.2485; Anal. Calcd for $(C_{48}H_{36}O_8)_1(CHCl_3)_{0.55}(H_2O)_{0.45}$: C 76.45, H 4.93, Cl 0.70. Found, C 76.13, H 4.82, Cl 0.67.

*5,10 - Bis({3' - bromo - [1,1' - biphenyl] - 3 - yl}) - 15,18,19,22 - tetraoxapentacyclo[12.4.4.0$^{1,14}$.0$^{2,7}$.0$^{8,13}$]docosa - 2(7),3,5,8(13),9,11 - hexaene (Precursor **3f**)*:

Following the procedure to prepare **3a**, a reaction mixture of **2b** (548 mg, 1.00 mmol) and **1c** (1.56 g, 5.00 mmol) afforded the title compound in 65% yield (497 mg, 0.655 mmol) as a white solid. $R_f$ = 0.52 (chloroform); $^1$H NMR (600 MHz, $CDCl_3$) $\delta$ 8.18 (d, $J$ = 1.6 Hz, 2H), 7.88 (d, $J$ = 7.8 Hz, 2H), 7.79-7.78 (m, 4H), 7.69 (dd, $J$ = 7.8, 1.6 Hz, 2H), 7.65 (ddd, $J$ = 7.2, 1.5, 1.5 Hz, 2H), 7.59-7.54 (m, 6H), 7.50 (d, $J$ = 8.1 Hz, 2H), 7.32 (dd, $J$ = 8.1, 7.8 Hz, 2H), 4.28 (brs, 4H), 3.75 (brs, 4H); $^{13}$C{$^1$H} NMR (150 MHz, $CDCl_3$) $\delta$ 143.3, 143.0, 141.8, 140.6, 133.5, 132.4, 130.6, 130.5, 130.5, 129.6, 128.2, 127.1, 127.1, 126.7, 126.4. 126.0, 123.2, 123.1, 92.8, 61.6; HRMS (APCI/TOF) $m/z$ [M + H]$^+$ calcd for $C_{42}H_{31}Br_2O_4$ 757.0584, found 757.0586.

*27,30,39,42 - Tetraoxadecacyclo[20.12.4.4$^{26,31}$.1$^{2,6}$.1$^{7,11}$.1$^{12,16}$.1$^{17,21}$.0$^{25,37}$.0$^{26,31}$.0$^{32,36}$]hexatetraconta - 1(35),2(46),3,5,7,9,11(45),12(44),13,15,17,19,21(43),22(38),23,25(37),32(36),33 - octadecaene (Macrocycle **4f**)*: Following the reaction procedure to prepare **4a**, the macrocyclization of **3f** (200 mg, 0.264 mmol) afforded the title compound in 34% yield (55 mg, 0.091 mmol) as a white solid after the purification by recrystallization from *o*-dichlorobenzene. $^1$H NMR (600 MHz, $CDCl_3$) $\delta$ 8.70 (s, 2H), 8.44 (dd, $J$ = 1.8, 1.8 Hz, 2H), 8.40 (dd, $J$ = 1.8, 1.2 Hz, 2H), 7.90-7.87 (m, 4H), 7.81-7.77 (m, 4H), 7.76-7.73 (m, 4H), 7.60 (dd, $J$ = 7.8, 7.8 Hz, 2H), 7.59 (dd, $J$ = 7.8, 7.8 Hz, 2H), 4.29 (brs, 4H), 3.77 (brs, 4H); $^{13}$C{$^1$H} NMR (150 MHz, $CDCl_3$) $\delta$ 141.5, 141.4, 141.4, 140.9, 140.0, 133.7, 132.5, 129.7, 127.1, 126.8, 126.4, 126.3, 126.0, 125.7, 125.6, 125.4, 123.0, 93.0 (A signal of the carbon nuclei in the acetal group was not observed probably due to slow conformational change of the acetal group on the NMR timescale.); HRMS (APCI/TOF) $m/z$ [M + H]$^+$ calcd for $C_{42}H_{31}O_4$ 599.2217, found 599.2231; Anal. Calcd for $(C_{42}H_{30})_1(C_6H_4Cl_2)_{0.05}$: C 83.83, H 5.02, Cl 0.58. Found, C 83.65, H 5.13, Cl 0.29.

**Synthesis of Other Relevant Macrocycles.**

*7,10,21,24,35,38,47,50,53,56,61,64 - Dodecaoxahexadecacyclo[28.12.4.4$^{6,11}$.4$^{20,25}$.4$^{34,39}$.2$^{2,5}$.2$^{12,15}$.2$^{16,19}$.2$^{26,29}$.0$^{4,13}$.0$^{6,11}$.0$^{18,27}$.0$^{20,25}$.0$^{33,45}$.0$^{34,39}$.0$^{40,44}$]hexahexaconta - 1(43),2,4,12,14,16,18,26,28,30(46),31,33(45),40(44),41,51,57,59,65 -*

*octadecaene (Macrocycle **4g**)*: After stirring a mixture of 2,2'-bipyridine (6.50 g, 41.6 mmol), 1,5-cyclooctadiene (5.10 mL, 41.6 mmol) and bis(1,5-cyclooctadiene)nickel(0) (11.4 g, 41.6 mmol) in toluene (330 mL) and DMF (330 mL) at 80 ºC for 30 min, a solution of compound **1b** (9.00 g, 19.8 mmol) in toluene (1.32 L) was added dropwise over 1 h. The mixture was stirred at 80 °C for an additional 1 h. After the reaction mixture was cooled to ambient temperature, water (2 L) was added, and the mixture was stirred vigorously overnight. After extraction with toluene, the combined organic layer was washed with brine, dried over $Na_2SO_4$ and concentrated in vacuo. The crude material was purified by silica gel column chromatography (eluent: chloroform) and gel permeation chromatography. The material was washed with boiling PhCl (100 mL) and reprecipitated from $CHCl_3$/MeOH to give the title compound as a white solid in 27% yield (1.68 g, 1.78 mmol). $^1$H NMR (600 MHz, $CDCl_3$) $\delta$ 8.81 (d, $J$ = 1.5 Hz, 6H), 7.98 (dd, $J$ = 8.0, 1.5 Hz, 6H), 7.89 (d, $J$ = 8.0 Hz, 6H), 4.28 (brs, 12H), 3.76 (brs, 12H); $^{13}$C{$^1$H} NMR (150 MHz, $CDCl_3$) $\delta$ 139.7, 133.8, 133.1, 127.3, 126.1, 121.8, 92.9, 61.7; HRMS (APCI/TOF) $m/z$ $[M + H]^+$ calcd for $C_{54}H_{43}O_{12}$ 883.2749, found 883.2724; Anal. Calcd for $(C_{54}H_{42}O_{12})_1(CHCl_3)_{0.55}$: C 69.07, H 4.52, Cl 6.17. Found, C 68.88, H 4.47, Cl 5.82.

*1,6-Bis(6-bromophenanthren-3-yl)hexane (**5**)*: To a THF solution of 9-BBN (0.5 M; 0.500 mL, 0.250 mmol) was added 1,5-hexadiene (14.5 μL, 0.122 mmol) at ambient temperature, and the mixture was stirred for 2 h. This solution was then transferred to a mixture of 3,6-dibromophenanthrene (**1a**) (123 mg, 0.365 mmol) and $Pd(PPh_3)_4$ (123 mg, 7.30 μmol) in THF (2.5 mL) and 1.2 M NaOH aq. (0.6 mL, 0.730 mmol). After the reaction mixture was stirred at 65 ºC for 15 h, 1 M HCl aq. (4 mL) was added. The aqueous layer was extracted with $CHCl_3$, and the combined organic layer was washed with water (4 mL) and brine (4 mL), dried over $Na_2SO_4$, and concentrated in vacuo. The crude mixture was purified by gel permeation chromatography to give the title compound as a white solid in 31% yield (23 mg, 0.038 mmol). $^1$H NMR (600 MHz, $CDCl_3$) $\delta$ 8.80 (d, $J$ = 1.8 Hz, 2H), 8.36 (s, 2H), 7.80 (d, $J$ = 7.7 Hz, 2H), 7.73 (d, $J$ = 8.4 Hz, 2H), 7.72 (d, $J$ = 9.0 Hz, 2H), 7.66 (dd, $J$ = 8.4, 1.8 Hz, 2H), 7.62 (d, $J$ = 9.0 Hz, 2H), 7.46 (dd, $J$ = 7.7, 1.5 Hz, 2H), 2.88 (t, $J$ = 7.8 Hz, 4H), 1.79 (m, 4H), 1.49 (m, 4H); $^{13}$C{$^1$H} NMR (150 MHz, $CDCl_3$) $\delta$ 141.9, 131.8, 130.9, 130.6, 130.2, 129.7, 129.4, 128.7, 128.4,

127.4, 125.6, 125.5, 122.0, 120.7, 36.7, 31.9, 29.4; HRMS (APCI) *m/z* $[M + H]^+$ calcd for $C_{34}H_{29}Br_2$ 595.0631, found 595.0607.

*Heptacyclo[16.8.4.2$^{2,5}$.2$^{8,11}$.0$^{4,9}$.0$^{21,29}$.0$^{24,28}$]tetratriaconta-1(27),2,4,6,8,10,18(30),19,21(29),22,24(28),25,31,33-tetradecaene (Macrocycle **6**)*: A mixture of 2,2'-bipyridine (625 mg, 4.00 mmol), 1,5-cyclooctadiene (490 μL, 4.00 mmol) and bis(1,5-cyclooctadiene)nickel(0) (1.10 g, 4.00 mmol) in a mixture of toluene (8.3 mL) and DMF (8.3 mL) was stirred at 65 ºC for 30 min. A solution of compound **5** (278 mg, 0.466 mmol) in toluene (33.4 mL) was added dropwise to the mixture over 1 h, and the stirring was continued for an additional 1 h at 65 ºC. After the reaction mixture was cooled down to room temperature, 1 M HCl aq. (60 mL) was added, and the mixture was stirred vigorously overnight. The organic layer was washed with water (50 mL) and brine (50 mL), dried over $Na_2SO_4$, and concentrated in vacuo. The crude material was purified by silica gel column chromatography (eluent: chloroform) and gel permeation chromatography to afford the title compound as a white solid in 77% yield (156 mg, 0.357 mmol). $^1$H NMR (600 MHz, $CDCl_3$) $\delta$ 9.42 (d, $J$ = 1.4 Hz, 2H), 8.85 (s, 2H), 8.11 (dd, $J$ = 8.0, 1.4 Hz, 2H), 8.02 (d, $J$ = 8.0 Hz, 2H), 7.83 (d, $J$ = 8.0 Hz, 2H), 7.75 (s, 4H), 7.46 (dd, $J$ = 8.0, 1.5 Hz, 2H), 3.08 (t, $J$ = 6.6 Hz, 4H), 2.14 (m, 4H), 1.81 (m, 4H); $^{13}$C{$^1$H} NMR (150 MHz, $CDCl_3$) $\delta$ 140.1, 138.2, 131.6, 130.7, 130.4, 130.4, 129.1, 129.1, 128.4, 127.0, 125.6, 124.6, 121.8, 119.3, 34.2, 29.9, 27.8; HRMS (APCI/TOF) *m/z* $[M + H]^+$ calcd for $C_{34}H_{29}$ 437.2264, found 437.2254; Anal. Calcd for $C_{34}H_{28}$: C 93.54, H 6.46. Found, C 93.29, H 6.53.

**Theoretical Calculations.** The $S_0/S_1$-MECI geometries of [6]CMP and [3]CPhen$_{3,6}$ were searched by the following procedures. At the first, $S_{0MIN}$ geometries were systematically explored using SC-AFIR method[15] at the density-functional-based tight-binding (DFTB) level.[24] Four and two $S_{0MIN}$ geometries at the DFTB level were obtained for [6]CMP and [3]CPhen$_{3,6}$, respectively. To search for the guess geometries of $S_0/S_1$-MECIs, minimum energy seams of crossing geometries between the ground singlet and triplet electronic states ($S_0/T_1$ -MESXs) were explored[25] using the gradient projection (GP)/SC-AFIR method[14] at the DFTB level. In the $S_0/T_1$-MESX search, the initial

geometries were set to the $S_{0MIN}$ geometries at the DFTB level, and the model collision energy parameter for the SC-AFIR method was set to 100 kJ $mol^{-1}$.[26] This search automatically generates an extensive list of guess structures. Then, $S_0/T_1$-MESXs which were energetically higher than the lowest $S_0/T_1$-MESX by 1.0 eV or more were excluded from the list. The remaining $S_0/T_1$-MESXs were reoptimized to the $S_0/S_1$-MECI geometries using energy shift (ES)[27]/TDDFT approach with an ES value of 10.0 kJ/mol,[16] where the average value of $S_0$ and $S_1$ energies on each $S_0/S_1$-MECI is shown as the $S_0/S_1$-MECI energy in this paper.

As the next step, the internal conversion paths on the $S_1$ surface from $S_{1MIN}$ to $S_0/S_1$-MECI regions were explored using the double-sphere AFIR (DS-AFIR) method.[28] To determine the energetically most preferred $S_{1TS}$, the locally updated planes (LUP) method[29] was applied to all the obtained DS-AFIR paths. Finally, the energetically most preferred $S_{1TS}$, *i.e.* 5.24 eV for [6]CMP and 5.00 eV for [3]$CPhen_{3,6}$, were determined. The reaction path through the most preferred $S_{1TS}$ was verified by the intrinsic reaction coordinate (IRC) calculation. The ωB97XD functional[30] with the 6-31G(d) basis set (denoted by ωB97XD/6-31G(d)) was employed in DFT and TDDFT calculations, and the solvent effect of toluene was evaluated using conductor-like polarizable continuum model (CPCM).[31] In the TDDFT calculations, Tamm-Dancoff approximation (TDA)[32] was used.

To evaluate the $S_{1MIN}$ level shown in Figure 3, $S_{0MIN}$ geometries of each molecule were explored using the SC-AFIR method[15] at the DFTB[24] level. Then, $S_{1MIN}$ geometries were searched by optimizing the ten most stable $S_{0MIN}$ geometries at the TD-ωB97XD/6-31G(d) level. The solvent effects were considered using CPCM,[31] where toluene was adopted for [3]$CPhen_{3,6}$, **4a**, **4b**, **4c**, **4d**, **4g**, **6**, and phenanthrene while chloroform was used for [6]CMP, **4e** and **4f**. In Figure 3, the energy of the most stable $S_{1MIN}$ was shown relative to the most stable $S_{0MIN}$.

All the DFTB, DFT and TDDFT energies and gradients were computed using the Gaussian 09 and Gaussian 16 program packages.[33] Also, the explorations of $S_{0MIN}$, $S_{1TS}$ and $S_0/S_1$-MECI geometries were done using the developmental version of GRRM program.[34]

**Supporting Information.** The Supporting Information is available free of charge via the Internet at http://pubs.acs.org. Spectroscopic data, theoretical calculations, X-ray crystallography data and a CIF file for **4a**.

**Acknowledgement.** This study is partly supported by JST ERATO (JPMJER1301), JST PRESTO (JPMJPR16N8), JST CREST (JPMJCR14L5) and KAKENHI (17H01033, 17K05772). We thank Dr. M. Oinuma and Dr. S. Takahashi for the synthesis of precursors. A part of the results was computed at the computer center of Kyoto University. We were granted access to the X-ray diffraction instruments in SPring-8 BL38B1 beamline (no. 2017B1301).

**References**

(1) Iyoda, M.; Yamakawa, J.; Rahman, M. J. Conjugated macrocycles: Concepts and applications. *Angew. Chem. Int. Ed.* **2011**, *50*, 10522-10553.

(2) Sato, S.; Yoshii, A.; Takahashi, S.; Furumi, S.; Takeuchi, M.; Isobe, H. Chiral intertwined spirals and magnetic transition dipole moments dictated by cylinder helicity. *Proc. Natl. Acad. Sci. U.S.A.* **2017**, *114*, 13097-13101.

(3) Pham, S.-T.; Ikemoto, K.; Suzuki, K. Z.; Izumi, T.; Taka, H.; Kita, H.; Sato, S.; Isobe, H.; Mizukami, S. Magneto-electroluminescence effects in the single-layer organic light-emitting devices with macrocyclic aromatic hydrocarbons. *APL Mater.* **2018**, *6*, 026103.

(4) (a) Xue, J. Y.; Izumi, T.; Yoshii, A.; Ikemoto, K.; Koretsune, T.; Akashi, R.; Taka, H.; Kita, H.; Sato, S.; Isobe, H. Aromatic hydrocarbon macrocycles for highly efficient organic light-emitting devices with single-layer architectures. *Chem. Sci.* **2016**, *7*, 896-904. (b) Ikemoto, K.; Yoshii, A.; Izumi, T.; Taka, H.; Kita, H.; Xue, J. Y.; Kobayashi, R.; Sato, S.; Isobe, H. Modular synthesis of aromatic hydrocarbon macrocycles for simplified, single-layer organic light-emitting devices. *J. Org. Chem.* **2016**, *81*, 662-666.

(5) Izumi, T.; Tian, Y.; Ikemoto, K.; Yoshii, A.; Koretsune, T.; Arita, R.; Kita, H.; Taka, H.; Sato, S.; Isobe, H. Efficient blue electroluminescence from a single-layer organic device composed solely of hydrocarbons. *Chem. Asian J.* **2017**, *12*, 730-733.

(6) Tian, Y.; Ikemoto, K.; Sato, S.; Isobe, H. [*n*]Cyclo-3,6-phenanthrenylenes: Synthesis, structure, and fluorescence. *Chem. Asian J.* **2017**, *12*, 2093-2097.

(7) (a) Miyaura, N.; Yamada, K.; Suzuki, A. A new stereospecific cross-coupling by the palladium-catalyzed reaction of 1-alkenylboranes with 1-alkenyl or 1-alkyl halides. *Tetrahedron Lett.* **1979**, *20*, 3437-3440. (b) Miyaura, N.; Suzuki, A. Palladium-catalyzed cross-coupling reactions of organoboron compounds. *Chem. Rev.* **1995**, *95*, 2457-2483.

(8) (a) Yamamoto, T. Electrically conducting and thermally stable π-conjugated poly(arylene)s prepared by organometallic processes. *Prog. Polym. Sci*. **1992**, *17*, 1153-1205. (b) Yamamoto, T.; Hayashi, Y.; Yamamoto, A. A novel type of polycondensation utilizing transition metal-catalyzed C-C coupling. I. Preparation of thermostable polyphenylene type polymers. *Bull. Chem. Soc. Jpn.* **1978**, *51*, 2091-2097.

(9) (a) Staab, H. A.; Binnig, F. Synthese und eigenschaften von hexa-m-phenylen. *Tetrahedron Lett.* **1964**, 319-321. (b) Bräunling, H.; Binnig, F.; Staab, H. A. Alkyl-substituierte hexa- und octa-*m*-phenylene. *Chem. Ber.* **1967**, *100*, 880-888.

(10) (a) Nakanishi, W.; Yoshioka, T.; Taka, H.; Xue, J. Y.; Kita, H.; Isobe, H. [*n*]Cyclo-2,7-

naphthylenes: Synthesis and isolation of macrocyclic aromatic hydrocarbons having bipolar carrier transport ability. *Angew. Chem. Int. Ed.* **2011**, *50*, 5323-5326. (b) Xue, J. Y.; Ikemoto, K.; Takahashi, N.; Izumi, T.; Taka, H.; Kita, H.; Sato, S.; Isobe, H. Cyclo-*meta*-phenylene revisited: Nickel-mediated synthesis, molecular structures, and device application. *J. Org. Chem.* **2014**, *79*, 9735-9739.

(11) For the compounds with short absorption bands, we adopted $CHCl_3$ as the solvents, whereas, for the compounds with longer absorption bands, toluene was adopted as a non-polar solvent.

(12) (a) Bernardi, F.; Olivucci, M.; Robb, M. A. Potential energy surface crossings in organic photochemistry. *Chem. Soc. Rev.* **1996**, 25, 321-328. (b) Yarkony, D. R. Conical intersections: diabolical and often misunderstood. *Acc. Chem. Res.* **1998**, 31, 511-518. (c) Sobolewski, A. L.; Domcke, W.; Dedonder-Lardeux, C.; Jouvet, C. Excited-state hydrogen detachment and hydrogen transfer driven by repulsive 1πσ* states: A new paradigm for nonradiative decay in aromatic biomolecules. *Phys. Chem. Chem. Phys.* **2002**, 4, 1093-1100. (d) Levine, B. G.; Martinez, T. J. Isomerization through conical intersections. *Annu. Rev. Phys. Chem.* **2007**, 58, 613-634.

(13) Harabuchi, Y.; Taketsugu, T.; Maeda, S. Exploration of minimum energy conical intersection structures of small polycyclic aromatic hydrocarbons: toward an understanding of the size dependence of fluorescence quantum yields. *Phys. Chem. Chem. Phys.* **2015**, *17*, 22561-22565.

(14) (a) Harabuchi, Y.; Taketsugu, T.; Maeda, S. Combined gradient projection/single component artificial force induced reaction (GP/SC-AFIR) method for an efficient search of minimum energy conical intersection (MECI) geometries. *Chem. Phys. Lett.* **2017**, 674, 141-145. (b) Harabuchi, Y.; Saita, K.; Maeda, S. Exploring radiative and nonradiative decay paths in indole, isoindole, quinoline, and isoquinoline. *Photochem. Photobiol. Sci.* **2018**, *17*, 315-322.

(15) (a) Maeda, S.; Taketsugu, T.; Morokuma, K. Exploring transition state structures for intramolecular pathways by the artificial force induced reaction method. *J. Comput. Chem.* **2014**, *35*, 166-173. (b) Maeda, S.; Harabuchi, Y.; Takagi, M.; Taketsugu, T.; Morokuma, K. Artificial force induced reaction (AFIR) method for exploring quantum chemical potential energy surfaces. *Chem. Rec.* **2016**, *16*, 2232-2248.

(16) Harabuchi, Y.; Hatanaka, M.; Maeda, S. Exploring approximate geometries of minimum energy conical intersections by TDDFT calculations. *Chem. Phys. Lett. X* **2019**, *2*, 100007.

(17) Harabuchi, Y.; Taketsugu, T.; Maeda, S. Nonadiabatic pathways of furan and dibenzofuran: What makes dibenzofuran fluorescent? *Chem. Lett.* **2016**, *45*, 940-942.

(18) Shi, J.; Izquierdo, M. A.; Oh, S.; Park, S. Y.; Milián-Medina, B.; Roca-Sanjuán, D.; Gierschner, J. Inverted energy gap law for the nonradiative decay in fluorescent floppy molecules: larger fluorescence quantum yields for smaller energy gaps. *Org. Chem. Front.* **2019**, 6, 1948-1954.

(19) Nanosecond-order decays of the fluorescence were commonly observed with fluorescent

macrocycles (**4a**, **4b**, **4c** and **6**; Figure S2).

(20) Talele, H. R.; Gohil, M. J.; Bedekar, A. V. Synthesis of derivatives of phenanthrene and helicene by improved procedures of photocyclization of stilbenes. *Bull. Chem. Soc. Jpn.* **2009**, *82*, 1182-1186.

(21) BaniKhaled, M. O.; Mottishaw, J. D.; Sun, H. Steering power of perfluoroalkyl substituents in crystal engineering: Tuning the π-π distance while maintaining the lamellar packing motif for aromatics with various sizes of π-conjugation. *Cryst. Growth Des.* **2015**, *15*, 2235-2242.

(22) Hitosugi, S.; Nakamura, Y.; Matsuno, T.; Nakanishi, W.; Isobe, H. Iridium-catalyzed direct borylation of phenacenes. *Tetrahedron Lett.* **2012**, *53*, 1180-1182.

(23) Shibata, M.; Ito, H.; Itami, K. Oxidative homocoupling reaction of aryltrimethylsilanes by Pd/*o*-chloranil catalysis. *Chem. Lett.* **2017**, *46*, 1701-1704.

(24) Zheng, G.; Witek, H. A.; Bobadova-Parvanova, P.; Irle, S.; Musaev, D. G.; Prabhakar, R.; Morokuma, K.; Lundberg, M.; Elstner, M.; Köhler, C.; Frauenheim, T. Parameter calibration of transition-metal elements for the spin-polarized self-consistent-charge density-functional tight-binding (DFTB) method: Sc, Ti, Fe, Co, and Ni. *J. Chem. Theory Comput.* **2007**, *3*, 1349-1367.

(25) Suzuki, S.; Maeda, S.; Morokuma, K. Exploration of quenching pathways of multiluminescent acenes using the GRRM method with the SF-TDDFT method. *J. Phys. Chem. A* **2015**, *119*, 11479-11487.

(26) Maeda, S.; Harabuchi, Y.; Taketsugu, T.; Morokuma, K. Systematic exploration of minimum energy conical intersection structures near the Franck-Condon region. *J. Phys. Chem. A* **2014**, *118*, 12050-12058.

(27) Hatanaka, M.; Morokuma, K. Exploring the reaction coordinates for f-f emission and quenching of lanthanide complexes - Thermosensitivity of terbium(III) luminescence. *J. Chem. Theory Comput.* **2014**, *10*, 4184-4188.

(28) Maeda, S.; Harabuchi, Y.; Takagi, M.; Saita, K.; Suzuki, K.; Ichino, T.; Sumiya, Y.; Sugiyama, K.; Ono, Y. Implementation and performance of the artificial force induced reaction method in the GRRM17 program. *J. Comput. Chem.* **2018**, *39*, 233-250.

(29) Choi, C.; Elber, R. Reaction path study of helix formation in tetrapeptides: Effect of side chains. *J. Chem. Phys.* **1991**, *94*, 751-760.

(30) Chai, J. D.; Head-Gordon, M. Long-range corrected hybrid density functionals with damped atom-atom dispersion corrections. *Phys. Chem. Chem. Phys.* **2008**, 10, 6615-6620.

(31) Barone, V.; Cossi, M. Quantum calculation of molecular energies and energy gradients in solution by a conductor solvent model. *J. Phys. Chem. A* **1998**, *102*, 1995-2001.

(32) Hirata, S.; Head-Gordon, M. Time-dependent density functional theory within the Tamm-Dancoff approximation. *Chem. Phys. Lett.* **1999**, *314*, 291-299.

(33) Gaussian 16, Revision B.01, Frisch, M. J.; Trucks, G. W.; Schlegel, H. B.; Scuseria, G. E.; Robb, M. A.; Cheeseman, J. R.; Scalmani, G.; Barone, V.; Petersson, G. A.; Nakatsuji, H.; Li, X.; Caricato, M.; Marenich, A. V.; Bloino, J.; Janesko, B. G.; Gomperts, R.; Mennucci, B.; Hratchian, H. P.; Ortiz, J. V.; Izmaylov, A. F.; Sonnenberg, J. L.; Williams-Young, D.; Ding, F.; Lipparini, F.; Egidi, F.; Goings, J.; Peng, B.; Petrone, A.; Henderson, T.; Ranasinghe, D.; Zakrzewski, V. G.; Gao, J.; Rega, N.; Zheng, G.; Liang, W.; Hada, M.; Ehara, M.; Toyota, K.; Fukuda, R.; Hasegawa, J.; Ishida, M.; Nakajima, T.; Honda, Y.; Kitao, O.; Nakai, H.; Vreven, T.; Throssell, K.; Montgomery, Jr. J. A.; Peralta, J. E.; Ogliaro, F.; Bearpark, M. J.; Heyd, J. J.; Brothers. E. N.; Kudin, K. N.; Staroverov, V. N.; Keith, T. A.; Kobayashi, R.; Normand, J.; Raghavachari, K.; Rendell, A. P.; Burant, J. C.; Iyengar, S. S.; Tomasi, J.; Cossi, M.; Millam, J. M.; Klene, M.; Adamo, C.; Cammi, R.; Ochterski, J. W.; Martin, R. L.; Morokuma, K.; Farkas, O.; Foresman, J. B.; Fox, D. J. Gaussian, Inc., Wallingford CT, **2016**.

(34) Maeda, S.; Harabuchi, Y.; Sumiya, Y.; Takagi, M.; Suzuki, K.; Sugiyama, K.; Ono, Y.; Hatanaka, M.; Osada, Y.; Taketsugu, T.; Morokuma, K.; Ohno, K. GRRM, A developmental version ed.; Hokkaido University: Sapporo, 2019.